ELSEVIER

International Journal of Minerals, Metallurgy and Materials
Volume 16, Number 6, December 2009, Page 701

Materials

Preparation, characterization and photocatalytic activity of N-doped TiO_2 nanocrystals

Hong-tao Gao[1,2], *Jing Zhou*[1], *Dong-mei Dai*[1], *and Guang-jun Liu*[2]

1) College of Chemistry and Molecular Engineering, Qingdao University of Science & Technology, Qingdao 266042, China
2) Department of Chemistry, Jining University, Jining 273155, China
(Received 2008-12-07)

Abstract: N-doped TiO_2 nanocrystals were prepared using titanium alkoxide as precipitant with different proportional materials. The products were characterized by X-ray diffraction, scanning electron microscopy, transmission electron microscopy, and UV-vis diffuse reflectance spectra. It is confirmed experimentally that the photocatalytic activity of N-doped TiO_2 is much higher than that of Degussa P25, when used for the degradation of crystal violet. The degradation kinetics follows an apparent first-order reaction, which is consistent with a generally observed Langmuir-Hinshelwood mechanism. The doping of TiO_2 with nitrogen significantly increases the absorption in the region of visible light. The energy of the band gap of N-doped TiO_2 is 2.92 eV. The better performance of N-doped TiO_2 can be explained by the fact that it is also excited with longer-wavelength light.

Key words: photocatalyst; degradation; nitrogen doping; TiO_2 nanocrystals; visible light; crystal violet

[*This work was financially supported by the Outstanding Adult-Young Scientific Research Encouraging Foundation of Shandong Province (No.2008BS09016), the Nature Science Foundation of Shandong Province (No.Y2007B15) and the Scientific Research Program of Shandong Province Education Department, China (No.J06D55).*]

1. Introduction

Industrial dyestuffs, including textile dyes, are being recognized as an important environmental threat. Toxic metabolites are released into various aquatic environments, including fresh, recreational, processed, and reclaimed water. The presence of these toxins has both environmental and socioeconomic impacts [1]. The treatment of dye-containing wastewater by conventional methods, such as flocculation, reverse osmosis, and activated carbon adsorption, has drawbacks due to the increasing number of refractory materials found in wastewater effluents, difficulties in the complete removal of color, and expensiveness [2]. The advanced oxidation technologies, such as TiO_2-mediated photocatalysis [3] and photo-Fenton processes [4], have been investigated to degrade dye pollutants during the past few years [5-6].

Titanium dioxide is becoming an efficient photocatalyst for its strong oxidation activity [7-8]. It produces electron-hole pairs in ultraviolet light (200-400 nm), which initiates the formation of surface radicals capable of oxidizing adsorbed organic and biological pollutants [9-10]. The degradation of dye wastewater using TiO_2 as photocatalyst has been developed to meet the increasing demand of an effective wastewater treatment due to its easy handling and high efficiency [11-12]. However, the low photodegradation rates for many target pollutants block the practical and widespread use. Some studies have focused on TiO_2 modification to improve photocatalytic activity in recently years [13-14]. The studies on the preparation and properties of TiO_2 nanocrystalline have attracted extensive interests [15-16]. One aspect of this work was to increase the photocatalytic activity of TiO_2 in the near UV by doping elements, such as Fe, Zn, Sb, Sn, and Bi, [17-18]. The other aspect was to make significant shift of the absorption edge to the visible light region [19-20].

Doping elements into TiO_2 is an efficiency method to enhance the catalytic activity in the visible light region. It was reported that noble and transition metals,

Corresponding author: Hong-tao Gao, **E-mail:** gaohongtao@gmail.com
Also available online at www.sciencedirect.com

such as Pt, Ag, Au, and Nd, could decrease the recombination of photogenerated holes and electrons and promoted interfacial electron transfer [21-22]. Surface modification could greatly affect the adsorption of all reactants and reaction efficiency [23]. The factors relevant to surface properties of TiO_2, such as the surface acidity, defects, and ·OH groups, could give rise to remarkable influence on the chemical properties of photocatalyst [24-25]. Some nonmetal elements, such as N, P, S, and F, could be doped into the catalyst. Introduction of anionic dopants to TiO_2 also made it possible to achieve TiO_2 band gap narrowing [17, 27] and extended the optical absorption of TiO_2 [28]. Wang *et al*. studied photocatalytic degradation of phenol in N-doped TiO_2 suspensions with various light sources [29].

In this study, N-doped TiO_2 nanocrystals were synthesized and characterized by X-ray diffraction (XRD), scanning electron microscopy (SEM), transmission electron microscopy (TEM), and UV-vis diffuse reflectance spectra (DRS). The photocatalytic activity of N-doped TiO_2 was studied on the degradation of crystal violet (CV). It is indicted that the photocatalytic activity of N-doped TiO_2 is much higher than that of Degussa P25.

2. Experimental

2.1. Chemicals

Tetrabutyl titanate ($Ti(OBu)_4$, 98%), isopropanol (*i*-PrOH, 99.7%), *n*-butanol and hydrochloric acid (HCl, 36%) were purchased from Tianjin Reagent Chemicals Co., Ltd. Dodecylamine ($C_{12}H_{25}NH_2$) was purchased from Chemicals Reagent Shanghai Co., Ltd. Crystal violet (CV, its structure is given in Fig. 1) was purchased from Tianjin Jinke Fine Chemical Academe as available dyes. Degussa P25 titanium dioxide (ca. 80wt% anatase, 20wt% rutile; the Brunauer- Emmett-Teller (BET) area, ca. 55 $m^2 \cdot g^{-1}$; mean particle size, ca. 30 nm) was used as the comparative photocatalyst. Reagents were used as received without any further purification. The millipore filter (pore size of 0.45 μm) was purchased from Shanghai Xinya Co., Ltd. Deionized and doubly distilled water was used in this work.

2.2. Instruments and apparatus

All direct photocatalysis experiments were conducted using an SGY-I photochemical reactor (Stonetech. EEC Ltd. Nanjing, China). A quartz cylinder (ϕ50 mm×450 mm) filled with 500 mL sample solution was placed inside the reactor and illuminated with a 300 W high-pressure mercury lamp. A magnetic stirrer was located at the base so that a homogeneous TiO_2 suspension could be maintained throughout the reaction.

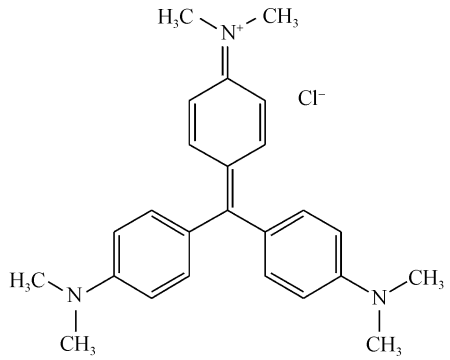

Fig. 1. Chemical structure of crystal violet.

The analysis instruments used in our work were as follows: Rigaku D/Max-rA diffractometer (Siemens) with Cu-K_α radiation; JEM-2000EX transmission electron microscopy; FESEN6700 scanning electron microscopy; UV-vis spectrophotometer (Varian Co., Cary50); solid-state UV-vis spectrophotometer (Varian Co., Cary500).

2.3. Experimental procedures

2.3.1. Preparation of N-doped TiO_2

Dodecylammoniumchloride micellar solution was stirred vigorously, which was made of dodecylamine, hydrochloric acid (36wt%) and pure water. Tetrabutyl titanate was dissolved in alcohol to form a titanium alkoxide precursor. And then it was added into the dodecylammoniumchloride micellar solution. Hydrolysis and condensation reactions of $Ti(OBu)_4$ occurred, forming a white turbid precipitate. The precipitate was condensed during drying at 35°C for 1 d, finally a white solid TiO_2/organic composite was formed. The composite was heat-treated in Muffle furnace to increase the crystallinity of TiO_2 and remove the dodecylammoniumchloride surfactant template. The solid TiO_2/organic composite was dried at 100°C for 1 h in an electric blast drying oven. After then, the samples were calcined at different temperatures (350°C or 550°C) for 3 h in a Muffle furnace, and cooled down naturally. Finally, the product of yellowish white N-doped TiO_2 was obtained.

2.3.2. Characterization

The powder XRD patterns of the catalysts were recorded on a RigakuD/Max-rA diffractometer with Cu-K_α radiation (λ=0.154059 nm). The crystallite size (*D*) was estimated from the width of lines in the XRD pattern according to the Scheerer formula:

$$D = K\lambda / \beta \cos\theta \quad (1)$$

where λ is the wavelength of the X-ray employed, β the full-width at half-maximum in radiation of the peak, θ the barge angle of the XRD peak, and K the Scherrer shape factor, K=0.9 [30].

JEM-2000EX transmission electron microscopy and FESEN6700 scanning electron microscopy were used to describe the particle size and morphology surface topography. The solid-state UV-visible spectrum was measured with a Cary500 spectrophotometer to describe the shifted absorption of the product.

2.3.3. Photocatalytic degradation of CV

The aqueous CV/TiO_2 dispersions were prepared by adding Degussa P25 titanium dioxide or N-doped TiO_2 (400 mg) to a 200-mL aqueous solution containing CV dye (40 mg/L). Prior to irradiation, the suspensions were magnetically stirred in the dark for about 40 min to ensure the establishment of a suitable adsorption-desorption equilibrium of the dye on the surface of TiO_2. The samples were irradiated under stirring by using a 300 W high-pressure mercury lamp, whose primary wavelength distribution was at 365 nm. At the given time intervals, 5-mL aliquots were sampled, centrifuged, and then filtered through a millipore filter (0.45 μm) to remove the TiO_2 particles. The filtrates were analyzed by a UV-vis spectrophotometer (Varian Co., Cary50) at 590 nm to record the temporal UV-vis spectral variations of the dyes. All experiments were carried out at room temperature. The absorption spectra were recorded and the rate of degradation was observed in terms of change in intensity at the maximal absorbance wavelength (λ_{max}) of CV. The extent of photo-decomposition was calculated using a calibrated relationship between the measured absorbance and its concentration, which could be seen in the following equation:

$$\ln\frac{C_0}{C} = \kappa t + b \tag{2}$$

where C_0 is the initial concentration of CV dye, $mg \cdot L^{-1}$; C the residual concentration of the dye, $mg \cdot L^{-1}$; t the reaction time; κ the slope; and b the intercept.

3. Results and discussion

3.1. Catalyst characterization

3.3.1. XRD analysis

The XRD patterns of the samples are shown in Fig. 2. The average crystallite size of the samples is about 20 nm, calculated according to Eq. (1). The XRD patterns of the products are different with different proportional materials in experimental condition. The crystalline phases of TiO_2 in different experimental conditions with various material proportions are listed in Table 1. As well known, titania has three different crystalline phases: anatase, rutile and brookite. Some studies confirmed that a mixture of anatase and rutile was more active than pure anatase [31]. However, other studies claimed that the anatase phase of titania was more active than rutile.

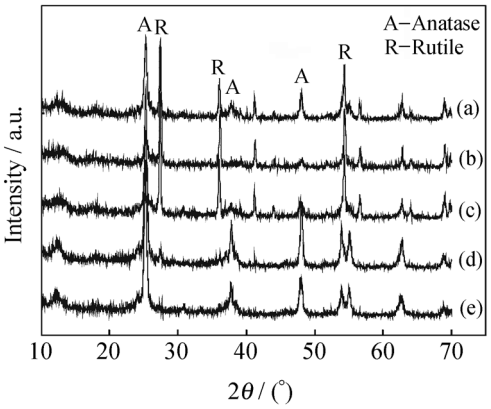

Fig. 2. XRD patterns of N-doped TiO_2.

Table 1. Crystalline phases of TiO_2 in different experimental conditions with various material proportions

Curve in Fig. 2	$Ti(OBu)_4$: $C_{12}H_{25}NH_2$: HCl : H_2O : C_4H_9OH (molar ratio)	Crystalline phase (anatase : rutile)
(a)	0.005 : 0.005 : 1 : 0.3 : 0.01	10.2wt% : 89.8wt%
(b)	0.01 : 0.01 : 1 : 0.3 : 0.01	26.6wt% : 73.4wt%
(c)	0.015 : 0.015 : 1 : 0.3 : 0.01	43.3wt% : 56.7wt%
(d)	0.005 : 0.005 : 1 : 0.3 : 0.02	89.2wt% : 10.8wt%
(e)	0.005 : 0.005 : 1 : 0.3 : 0.02 (isopropanol)	92.4wt% : 7.6wt%

The nanocrystallite phase of N-doped TiO_2 photocatalysts was identified by XRD, and there were two crystallite phases of anatase and rutile TiO_2 in samples, which can be seen in Fig. 2. Anatase peaks (25.2°) and rutile peaks (27.4°, 36.1° and 54.3°) of N-doped particles are observed in curves (a) and (b). And in curve (c), there appear anatase peaks (25.3°, 37.8° and 48.0°) and a rutile peak (27.4°). It shows that nanocrystallite phase varied according to material proportion, which can be seen in table 1. The source of nitrogen dopant had great effect on the crystal and structure of TiO_2. It could be summarized from the experimental results that the more amount of nitrogen resource ($C_{12}H_{25}NH_2$), the more anatase.

Another factor, which affects the structure and crystal of TiO_2, is titanium resource. The crystal phase, such as anatase and rutile, relies on the amount of $Ti(OBu)_4$. The proportion of anatase and rutile varies with the amount of $Ti(OBu)_4$. And the content of anatase increased as the $Ti(OBu)_4$ increases. More anatase TiO_2 appears when *i*-PrOH is replaced by *n*-butanol, as shown in curve (e) of Fig. 2, while the proportion of anatase TiO_2 in curve (d) is less. It perhaps resulted from the different alcohols of the two samples. Anatase peaks (25.2°, 37.8°, and 48.0°) are observed obviously in curve (e). However, both an anatase peak (25.2°) and rutile peaks (27.4°, 36.1° and 54.3°) are observed in curve (d).

In summary, the sample in curve (e) has the smallest particle size and the higher content of anatase. So the characters of the sample were compared with those of Degussa P25 in the following sections.

3.1.2. SEM and TEM analysis

Nitrogen doped TiO_2 was obtained with the crystallite size of about 20 nm according to XRD data. It is consistent with the crystallite size which can be seen in the SEM image (Fig. 3) and TEM image (Fig. 4). The presence of a disorder shell or incoherence within a particle can lead to such differences. The phase of anatase was reported the primary photocatalytic polymorph [31]. Degussa P25 has the relative proportions of the crystalline components to be 80wt% anatase and 20wt% rutile, while our synthetical product consists primarily of anatase (92.4wt%) and rutile (7.6wt%) (Table 1). So the products in our experiment might perform better for CV degradation.

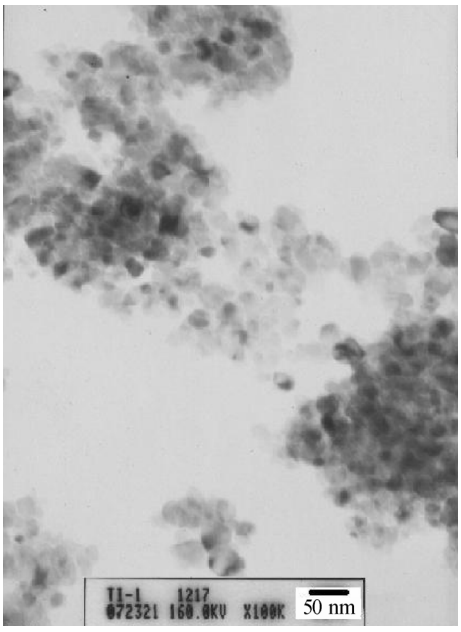

Fig. 3. TEM photograph of the N-doped TiO_2 particle.

3.1.3 UV-vis diffuse reflectance spectra analysis

Fig. 5 shows the DRS of N-doped TiO_2 and Degussa P25, respectively. It can be seen that the synthesized N-doped product shows increased absorption over a broad rand of 400-550 nm compared to Degussa P25. The energy gap (E_g) can be calculated for practical purposes by extrapolating a straight line to the abscissa axis from the DRS for both photocatalysts [32]. The observed E_g was 2.92 eV and 2.95 eV for the N-doped TiO_2 and the P25 respectively. The absorption shifting to the visible light region could be attributed to the modification of TiO_2 electronic structure due to the nitrogen dopant. It justified why it could be a potentially good candidate for performing photochemical reactions under visible light irradiation. It will be validated by experimental results in the next section.

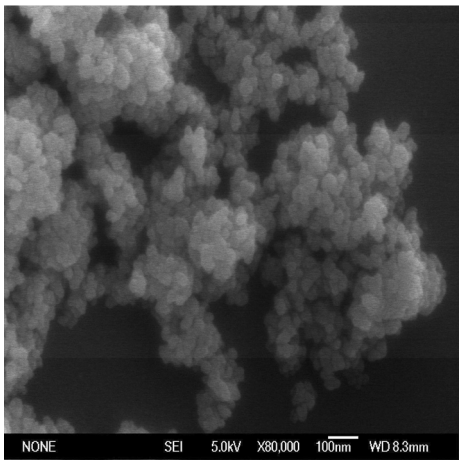

Fig. 4. SEM image of N-doped TiO_2 particles.

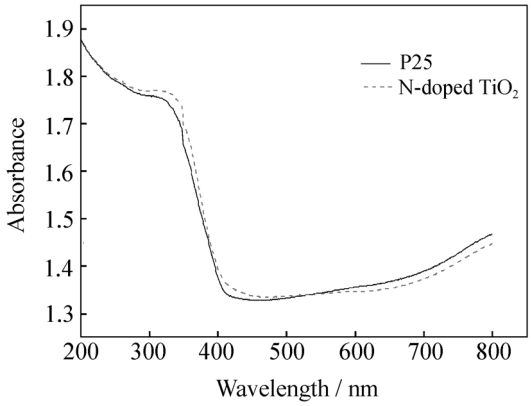

Fig. 5. Diffuse reflectance absorption spectra of P25 and N-doped TiO_2.

3.2. Photocatalytic activity of N-doped TiO_2

Fig. 6 shows the relationship between absorption and the irradiation time during the photocatalytic degradation of CV for P25 and N-doped TiO_2.

In Fig. 6(b), the absorption is very weak when the

irradiation time reaches 25 min. It is lower than that in Fig. 6(a) when the irradiation time is 55 min. The absorbances at 285, 301 and 590 nm are all very weak (near zero), when the irradiation time reaches 55 min. The CV decomposed almost completely by using N-doped TiO_2 as photocatalyst, when the irradiation time reached 1 h. It can be concluded that N-doped TiO_2 was prior to Degussa P25 in photocatalytic efficiency.

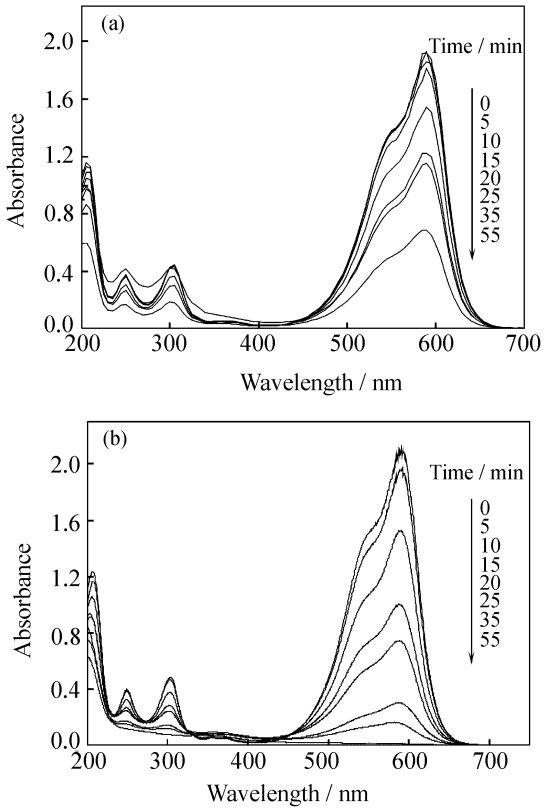

Fig. 6. Evolution of the UV-visible spectra of CV for various time intervals: (a) P25; (b) N-doped TiO_2.

The absorption at the maximal absorbance wavelength (590 nm) was chosen to evaluate the photocatalytic activity of catalysts. The kinetics of CV decomposition can be obtained by plotting the logarithm of C_0/C against irradiation time according to Eq. (2), which is shown in Fig. 7. Fairly good linear relationships are observed, indicating that all reactions follow the first-order kinetics. Thus slopes of the plot will yield the apparent fist-order rate constant, which can be used to assess the influence of the catalyst on the overall reaction rate. The constant is 0.09472 min^{-1} for N-doped TiO_2 and 0.01912 min^{-1} for Degussa P25, respectively, which indicate a faster dye decomposition and a higher catalytic activity for N-doped TiO_2. The better performance of N-doped TiO_2 could be explained by the fact that it was also excited with longer-wavelength light.

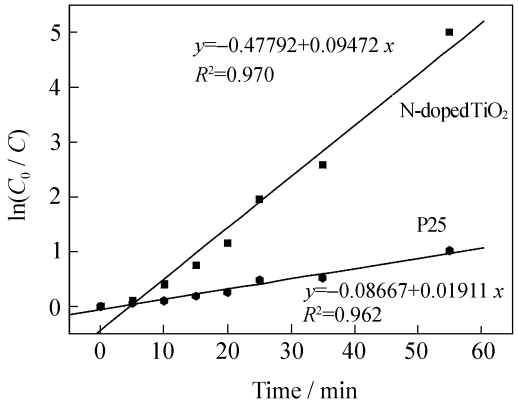

Fig. 7. First-order kinetic plots of CV degradation with different photocatalysts.

4. Conclusions

(1) The crystal phase of N-doped TiO_2 has relation to the nitrogen dopant and the proportion of the reaction materials. The content of anatase crystal phase varies with the amount of dopants.

(2) Compared with Degussa P25, the absorption band edge of N-doped TiO_2 shifts to a higher wavelength, indicating a better photocatalytic activity in the visible light region.

(3) The doping of TiO_2 with nitrogen significantly enhanced the photocatalytic efficiency. The better performance of the N-doped nanoparticles can be explained by the fact that it is also excited with longer-wavelength light.

References

[1] X.L. Dong, W. Ding, X.F. Zhang, and X.M. Liang, Mechanism and kinetics model of degradation of synthetic dyes by UV–vis/H_2O_2/Ferrioxalate complexes, *Dyes Pigm.*, 74(2007), No.2, p.470.

[2] M. Faisal, M.A. Tariq, and M. Muneer, Photocatalysed degradation of two selected dyes in UV-irradiated aqueous suspensions of titania, *Dyes Pigm.*, 72(2007), No.2, p.233.

[3] K. Selvam, M. Muruganandham, N. Sobana, and M. Swaminathan, Enhancement of UV-assisted photo-Fenton degradation of reactive orange 4 using TiO_2-P25 nanoparticles, *Sep. Purif. Technol.*, 54(2007), No.2, p.241.

[4] C.H. Wu and J.M. Chern, Kinetics of photocatalytic decomposition of methylene blue, *Ind. Eng. Chem. Res.*, 45(2006), No.19, p.6450.

[5] M.S. Lucas and J.A. Peres, Decolorization of the azo dye reactive black 5 by Fenton and photo-Fenton oxidation, *Dyes Pigm.*, 71(2006), No.2, p.236.

[6] H.L. Zheng and X.Y. Xiang, Oxidation of acidic dye Eosin Y by the solar photo-Fenton processes, *J. Hazard. Mater.*, 141(2007), No.3, p.457.

[7] S.U.M. Khan, M. Al-Shahry, and W.B. Ingler, Efficient photochemical water splitting by a chemically modified nTiO_2, *Science*, 297(2002), No.5590, p.2243.

[8] J.J. Zou, C.J. Liu, K.L. Yu, D.G. Cheng, Y.P. Zhang, F. He, H.Y. Du, and L. Cui, Highly efficient Pt/TiO_2 photocatalyst prepared by plasma-enhanced impregnation method, *Chem. Phys. Lett.*, 400(2004), No.4-6, p.520.

[9] W.W. Dunn, Y. Aikawa, and A.J. Bard, Characterization of particulate titanium dioxide photocatalysts by photoelectrophoretic and electrochemical measurements, *J. Am. Chem. Soc.*, 103(1981), No.12, p.3456.

[10] T. Takata, A. Tanaka, M. Hara, J.N. Kondo, and K. Domen, Recent progress of photocatalysts for overall water splitting, *Catal. Today*, 44(1998), No.1-4, p.17.

[11] C.H. Lee and J.Y. Yoon, Application of photoactivated periodate to the decolorization of reactive dye: reaction parameters and mechanism, *J. Photochem. Photobiol. A*, 165(2004), No.1, p.35.

[12] K. Nagaveni, G. Sivalingam, M.S. Hegde, and Girihar Madras, Photocatalytic degradation of organic compounds over combustion-synthesized nano-TiO_2, *Environ. Sci. Technol.*, 38(2004), No.5, p.1600.

[13] V.Subramanian, E. Wolf, and P.V. Kamat, Semiconductor-metal composite nanostructures. To what extent do metal nanoparticles improve the photocatalytic activity of TiO_2 films? *J. Phys. Chem. B*, 105(2001), No.46, p.11439.

[14] Y.B. Xie and C.W. Yuan, Photocatalysis of neodymium ion modified TiO_2 sol under visible light irradiation, *Appl. Surf. Sci.*, 221(2004), No.1-4, p.17.

[15] R. Asahi, T. Morikawa, T. Ohwaki, K. Aoki, and Y. Taga, Visible-light photocatalysis in nitrogen-doped titanium oxides, *Science*, 293(2001), No.13, p.269.

[16] Y. Ou, J.D. Lin, H.M. Zou, and D.W. Liao, Effects of surface modification of TiO_2 with ascorbic acid on photocatalytic decolorization of an azo dye reactions and mechanisms, *J. Mol. Catal. A*, 241(2005), No.1-2, p.59.

[17] E. Piera, M.I. Tejedor-Tejedor, M.E. Zorn, and M.A. Anderson, Relationship concerning the nature and concentration of Fe(III) species on the surface of TiO_2 particles and photocatalytic activity of the catalyst, *Appl. Catal. B*, 46(2003), No.4, p.671.

[18] Z. Yuan, J. Jia, and L. Zhang, Influence of co-doping of Zn(II)+Fe(III) on the photocatalytic activity of TiO_2 for phenol degradation, *Mater. Chem. Phys.*, 2(2002), No.2-3, p.323.

[19] H. Irie, Y. Watanabe, and K. Hashimoto, Nitrogen-concentration dependence on photocatalytic activity of $TiO_{2-x}N_x$ powders, *J. Phys. Chem. B*, 107(2003), No.23, p.5483.

[20] C. Burda, Y. Lou, X. Chen, A.C.S. Samia, J. Stout, and J.L. Gole, Enhanced nitrogen doping in TiO_2 nanoparticles, *Nano Lett.*, 3(2003), No.8, p.1049.

[21] R.J. Tayade, R.G. Kulkarni, and R.V. Jasra, Transition metal ion impregnated mesoporous TiO_2 for photocatalytic degradation of organic contaminants in water, *Ind. Eng. Chem. Res.*, 45(2006), No.15, p.5231.

[22] Y.X. Chen, S.Y. Yang, and K. Wang, Role of primary active species and TiO_2 surface characteristic in UV-illuminated photodegradation of Acid Orange 7, *J. Photochem. Photobiol. A*, 172(2005), No.1, p.47.

[23] H. Park and W. Choi, Effects of TiO_2 surface fluorination on photocatalytic reactions and photoelectrochemical behaviors, *J. Phys. Chem. B*, 108(2004), No.13, p.4086.

[24] D. Li, H. Haneda, S. Hishita, N. Ohashi, and N.K. Labhsetwar, Fluorine-doped TiO_2 powders prepared by spray pyrolysis and their improved photocatalytic activity for decomposition of gas-phase acetaldehyde, *J. Fluorine Chem.,* 126(2005), No.1, p.69.

[25] Y.T. Kwon, K.Y. Song, W.I. Lee, G.J. Choi, and Y.R. Do, Photocatalytic behavior of WO_3-loaded TiO_2 in an oxidation reaction, *J. Catal.*, 191(2000), No.1, p.192.

[26] V. Keller, P. Bernhardt, and F, Grain, Photocatalytic oxidation of butyl acetate in vapor phase on TiO_2, Pt/TiO_2 and WO_3/TiO_2 catalysts, *J. Catal.*, 215(2003), No.1, p.129.

[27] L. Kangle and Y.M. Xu, Effects of polyoxometalate and fluoride on adsorption and photocatalytic degradation of organic dye X3B on TiO_2: The difference in the production of reactive species, *J. Phys. Chem. B*, 110(2006), No.12, p.6204.

[28] J.W. Tang, H.D. Quan, and J.H. Ye, Photocatalytic properties and photoinduced hydrophilicity of surface-fluorinated TiO_2, *Chem. Mater.*, 19(2007), No.1, p.116.

[29] Z.P. Wang, W.M. Cai, X.T. Hong, X.L. Zhao, F. Xu, and C.G. Cai, Photocatalytic degradation of phenol in aqueous nitrogen-doped TiO_2 suspensions with various light sources, *Appl. Catal. B*, 57(2005), No.3, p.223.

[30] T. L´opez, M. Alvarez, F. Tzompantzi, and M. Picquart, Photocatalytic degradation of 2,4-dichlorophenoxiacetic acid and 2,4,6-trichlorophenol with ZrO_2 and Mn/ZrO_2 sol-gel materials, *J. Sol Gel Sci. Technol.*, 37(2006), No.3, p.207.

[31] O. Carp, C.L. Huisman, and A. Reller, Photoinduced reactivity of titanium dioxide, *Prog. Solid State Chem.*, 32(2004), No.1-2, p.33.

[32] S. Madhavi and W. Tim, Degradation of methylene blue by three-dimensionally ordered macroporous titania, *Environ. Sci. Technol.*, 41(2007), No.12, p.4405.

[33] T. Lopez and R. Gomez, Photocatalytic activity in the 2,4-dinitroaniline decomposition over TiO_2 sol-gel derived catalysts, *J. Sol Gel Sci. Technol.*, 22(2001), No.1-2, p.99.